Available online at www.sciencedirect.com
ScienceDirect
Bioelectrochemistry 69 (2006) 209–215
Bioelectrochemistry
www.elsevier.com/locate/bioelechem

Differential effects of plasma membrane electric excitation on H^+ fluxes and photosynthesis in characean cells

Alexander A. Bulychev *, Natalia A. Kamzolkina

Department of Biophysics, Faculty of Biology, Moscow State University, Moscow 119992, Russia

Received 16 February 2006; accepted 9 March 2006
Available online 19 April 2006

Abstract

Cells of characean algae exposed to illumination arrange plasma-membrane H^+ fluxes and photosynthesis in coordinated spatial patterns (bands). This study reveals that H^+ transport and photosynthesis patterns in these excitable cells are affected not only by light conditions but also by electric excitation of the plasma membrane. It is shown that generation of action potential (AP) temporally eliminates alkaline bands, suppresses O_2 evolution, and differentially affects primary reactions of photosystem II (PSII) in different cell regions. The quantum yield of PSII electron transport decreased after AP in the alkaline but not in acidic cell regions. The effects of electric excitation on fluorescence and the PSII electron flow were most pronounced at light-limiting conditions. Evidence was obtained that the shift in chlorophyll fluorescence after AP is due to the increase in ΔpH at thylakoid membranes. It is concluded that the AP-triggered pathways affecting ion transport and photosynthetic energy conversion are linked but not identical.

Keywords: *Chara corallina*; Action potential; Proton transport; Acidic and alkaline zones; Chloroplasts; Nonphotochemical quenching; Spatial heterogeneity

1. Introduction

Electrical excitation occurs in many plant cells but its physiological consequences are not yet fully recognized. The well-known examples are leaf movements triggered by action potentials (AP) in *Mimosa* and insectivorous plants [1,2]. Cells of some liverworts, algae, and vascular plants generate AP in response to light, chilling, burning, as well as chemical, mechanical, and electric stimuli [3–8]. These signals are thought to initiate responses of cells and organisms to injury or environmental changes [9]. Like in animals, AP in plants are caused by a regenerative voltage-dependent process of ion channel opening–closing and exhibit threshold phenomena [10,11]. Recent findings showed that propagating electric signals in mimosa leaves result in transient suppression of photosynthesis [12].

Internodal cells of characean algae represent a convenient model for studying plant cell excitability. This model allowed researchers to identify Ca^{2+}, Cl^-, and K^+ fluxes through ionic channels during AP generation [10,11,13,14] and to characterize the electrogenic H^+ pump of the plasma membrane (PM) [15]. Owing to large cell dimensions and fixed single-layer alignment of chloroplasts, the internodes of Characeae are convenient for exploring interactions between electric excitation, photosynthesis, and ion transport. Characean cells are known to form under light alternating subcellular domains with H^+ extrusion and H^+ sink activities that account for pH banding [16–19] and photosynthetic patterns [20–22]. Although the pH banding phenomenon is known for years, its regulation and associated metabolic patterns are poorly characterized. In addition to photosynthesis pattern, inhomogeneous distribution of mitochondria was observed in illuminated cells [23]. Cell regions with active photosynthesis accumulate mitochondria, whereas regions with low photosynthetic activity were depleted in these.

The pH pattern is strikingly influenced by AP generation [24]. A single AP produces a long-lasting suppression of the banding profile, which implies either involvement of a signaling cascade or a powerful side effect of cell excitation.

* Corresponding author. Tel.: +7 95 939 3503; fax: +7 95 939 1115.
E-mail address: bulychev@biophys.msu.ru (A.A. Bulychev).

1567-5394/$ - see front matter © 2006 Elsevier B.V. All rights reserved.
doi:10.1016/j.bioelechem.2006.03.001

Analysis of the chlorophyll fluorescence of photosystem II (PSII) in different cell domains revealed excitation-induced changes that were dissimilar for alkaline and acid regions. The AP-induced phenomena were tentatively assigned to the rise in cytosolic Ca^{2+} ($[Ca^{2+}]_{cyt}$) during excitation. The excitation-induced events at PM (suppression of counter-directed H^+ flows) and in chloroplasts (changes in PSII quantum yield of electron flow) remain largely unexplored to date. It is not known whether these processes have similar light requirements and if they are strictly linked or can proceed separately.

The aim of this work was to examine effects of PM excitation on transmembrane H^+ fluxes, effective quantum yield of PSII electron flow, and fluorescence quenching in subcellular domains of *Chara* internodes at various light intensities. This was achieved by monitoring external pH near the cell surface (pH_o) with a microprobe and by measuring photosynthetic activity of small cell regions with microfluorometry, saturation pulse method, and amperometric pO_2 sensor. These methods were previously employed to study light-dependent formation of photosynthetic and pH bands [21,22].

2. Materials and methods

Chara corallina internodes about 6 cm in length and 0.9 −1 mm in diameter without apparent calcium depositions were excised and placed in the medium containing 0.1 mM KCl, 1.0 mM NaCl, and 0.5 mM $CaCl_2$ (pH 6.8−7.2). A transparent chamber with the cell was mounted on a stage of Axiovert-25 CFL inverted microscope (Carl Zeiss, Germany) equipped with a Microscopy PAM fluorometer (Walz, Effeltrich, Germany).

Cell regions of H^+ extrusion and H^+ influx were detected with pH microelectrodes having tip diameter of 10–20 μm [22]. The terms “alkaline and acid cell regions” denote cell parts producing zones of high and low pH_o, respectively. The potential difference across PM was measured with capillary microelectrodes filled with 1 M KCl.

Chlorophyll fluorescence was measured on small (diameter 100 μm) portions of a chloroplast layer with a Microscopy-PAM fluorometer [25] and WinControl program (Walz). The pH probe was positioned within the fluorometric window. Low-intensity measuring light had no actinic effect, as evidenced by high ratios of variable to maximum fluorescence ($\Delta F/F_m$). Actinic light was directed from the upper light source of an Axiovert microscope. The highest fluence rates (PAR) were 150 and 30 μmol m^{-2} s^{-1} for white light and blue light (a cut-off glass filter, $\lambda < 580$ nm), respectively. Neutral glass filters were used for attenuating photon flux density. A black screen with a small ($d = 2.5$ mm) opening was placed 3 mm above the cell to ensure local actinic illumination; it shielded the whole cell except for a small region coaxial with the microscopic field of view.

The effective quantum yield of PSII electron flow ($\Delta F/F_m'$) and the coefficient of nonphotochemical quenching (NPQ) were estimated from equations $\Delta F/F_m' = (F_m' - F)/F_m'$ and $NPQ = (F_m - F_m')/F_m'$. Here F_m and F_m' designate maximal yields of fluorescence induced with a saturation pulse in a dark-adapted cell and in a cell exposed to actinic light, respectively, and F is actual fluorescence yield in the actinic light.

Changes in local O_2 content were measured with glass-insulated open Pt electrode having a tip diameter of 100 μm [21]. With the potential of Pt cathode of 0.65 V with respect to Ag/AgCl electrode, the stationary electrode current proportional to O_2 content was fed into a current-voltage converter with a transfer coefficient of $3 \cdot 10^7$ V/A.

The cell excitation was elicited by a rectangular pulse of transcellular electric current (~ 10 μA, 150 ms) passing through external electrodes [24]. Experiments were performed at least in triplicates. Figures display results of representative experiments. Bars in Fig. 3 show mean values and standard errors.

3. Results

3.1. Kinetics of pH and membrane potential changes induced by excitation and darkness

It was previously established that the light-dependent pH pattern along *Chara* cell transiently disappears after cell excitation [24]. The smoothing of pH_o profile was manifested as a slight pH rise in acidic zones and a large pH decrease in the alkaline zones. Large pH shifts in the alkaline zones are particularly convenient for exploring interactions between excitation and light-controlled pH banding.

Fig. 1a compares local pH changes induced in the alkaline zone by AP and darkening. The cell was first exposed to darkness at time $t = 0$, which led to the vanishing of the alkaline band after a lag period (solid line 1). The kinetics of pH decay was fit to a sigmoid curve shown with symbols. When the alkaline band recovered after returning continuous light, AP was triggered (curve 2). The AP-induced decrease in pH followed an exponential kinetics with one or (sometimes) two exponential terms. The dark- and excitation-induced pH changes had comparable amplitudes and decay rates; however, the AP-induced pH drop started without a lag period. Remarkably, the AP-induced decrease in pH_o was also observed if the electric stimulus was applied 30 s after darkening, i.e., during the lag phase of the sigmoid decay curve (results not shown). Even in this case, the AP-triggered pH decline started earlier than the response to darkness. The above similarities in AP- and dark-induced pH changes point to the involvement of a common factor in excitation-induced and dark-induced permeability changes of PM.

Fig. 1b displays the membrane potential (MP) records, made from the cytoplasm of alkaline cell region, upon dark–light transitions and after AP generation. Turning off the actinic light caused a large hyperpolarization of PM, while the transfer of cell to light repolarized the membrane after a transient hyperpolarization (curve 1). This temporal pattern is similar to light-induced MP changes in *C. corallina* observed previously [26]. Our experiment was extended by triggering AP in the light. In Fig. 1b, the dark- and AP-induced responses are overlaid. The cell excitation induced a large after-potential (curve 2) comparable in extent and time range to the dark-induced hyperpolarization. It is seen that the hyperpolarization

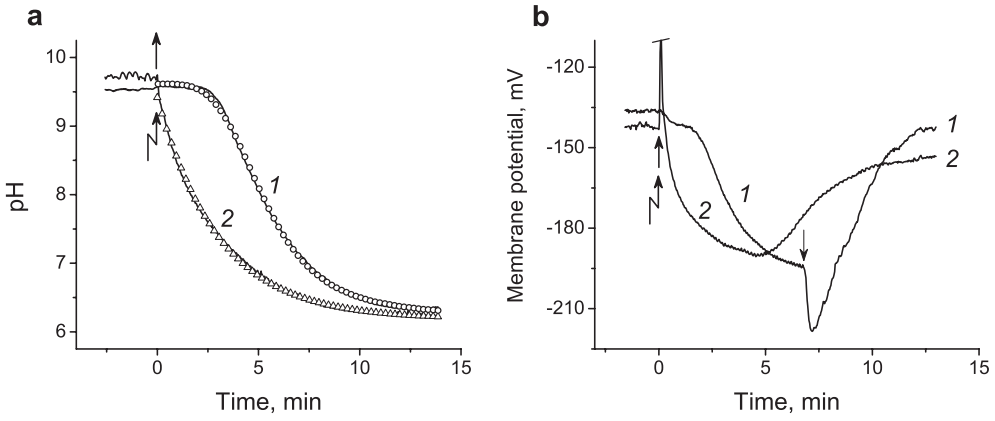

Fig. 1. Kinetics of pH and membrane potential changes in the alkaline zone of *C. corallina* cell upon darkening (1) and cell excitation (2). (a) Time-shifted kinetics of pH decay in the alkaline band caused by (1) light–dark transition at $t=0$ and (2) electrically stimulated AP generation in the light. Record 1 was fit to a sigmoid curve (round symbols): $pH_t=pH_2+(pH_1-pH_2)/(1+(t/t^*)^p)$, where $t^*=5.3$ min is the half-decay time, and p is a coefficient determining the shape and steepness of the sigmoid curve. Curve 2 was fit to a single exponential term with a half-decay time $t_{1/2}=1.84$ min (triangle symbols). (b) Membrane potential changes recorded from the cytoplasm of alkaline cell region upon two treatments: (1) darkening at $t=0$ and (2) AP generation in the light. Upward and downward arrows mark the moments when light was switched off and on during record 1, and zig-zag arrows mark AP generation. Only a part of AP is shown.

developed faster after AP than after light–dark transition. Fig. 1a and b reveals clear analogies in patterns of pH and MP changes after AP and light–dark transition. The responses induced by AP and darkness had similar magnitudes and comparable time scales, with a notable difference that AP-induced responses developed without the lag period.

3.2. Effects of cell excitation on chloroplast functioning in subcellular domains

The cell excitation decreases chlorophyll fluorescence and effective quantum yield of PSII electron flow $\Delta F/F_m'$ in specific cell areas [24]. In order to clarify whether AP-induced changes in F_m' and $\Delta F/F_m'$ result directly from the cessation of H^+ fluxes across PM, we examined relations between pH and PSII activity after AP in different cell regions (Fig. 2). The AP generation caused a substantial drop of F_m' and $\Delta F/F_m'$ in the alkaline cell regions (Fig. 2a), which was paralleled by the decrease in pH_o. In the acidic cell regions, the AP generation produced no significant changes in F_m' and $\Delta F/F_m'$ (Fig. 2b); the local pH_o increased after AP but this increase was small or negligible.

We compared the influence of AP with the effects of other treatments affecting alkaline bands, such as darkening and transition from overall to local illumination (Fig. 2c, d). Upon these treatments, the decay of alkaline peak was accompanied by the increase in both $\Delta F/F_m'$ and F_m', which was opposite to $\Delta F/F_m'$ and F_m' changes observed after AP. While the rise in $\Delta F/F_m'$ and F_m' on darkening is well known, the increase in these parameters after transfer to local illumination of equal intensity is remarkable and consistent with the notion that photosynthesis is more active in acidic than in alkaline cell regions [21]. The chloroplast movement can be excluded as chloroplasts in *Chara* are fixed in a rigid array. Thus, the pH_o lowering could occur alongside with inhibition and stimulation of photosynthesis at a constant irradiance of the area examined. Hence, the cessation of effective H^+ influx after AP cannot directly account for the changes in $\Delta F/F_m'$ and F_m'.

3.3. Light dependence of AP-induced changes in F_m' and $\Delta F/F_m'$ in relation to thylakoid ΔpH

The AP-induced responses of plasmalemma (pH_o changes) and chloroplasts ($\Delta F/F_m'$ and F_m' changes) differed strikingly in light requirements. Fig. 3a shows that triggering AP in the light induced a transient decrease in $\Delta F/F_m'$ (curve 1, open symbols). However, when AP was triggered 10 s after darkening, it had no effect on $\Delta F/F_m'$ in the same cell region (curve 2), even though it promoted dissipation of alkaline band (curve 3). The reaction pathways leading to AP-triggered changes in pH_o and $\Delta F/F_m'$ seem to arise from AP as a common cause but diverge at later stages of signal transduction.

Excitation-induced changes in F_m' and $\Delta F/F_m'$ were best pronounced at light-limiting conditions that did not cause nonphotochemical quenching. Fig. 3b shows that cell excitation at low irradiance induced a large decrease in F_m', shifting it close to the level established in high light. When the light intensity was raised to 30 μmol m^{-2} s^{-1}, the steady-state F_m' level lowered, reflecting strong nonphotochemical quenching; in this case AP had little effect on F_m'. This points to complementary relations between AP-induced and light-induced quenching. Fig. 3c displays the relations between stationary level of nonphotochemical quenching (NPQ) and the AP-induced decrease in F_m'. The increase in light intensity elevated NPQ and diminished the AP-induced F_m' changes.

Nonphotochemical quenching (a mechanism converting the excess chlorophyll excitations to heat) results from several causes, including transthylakoid pH gradient (ΔpH) and zeaxanthin accumulation, state transitions, and photoinhibition [27,28]. In order to test if nonphotochemical quenching in *Chara* is ΔpH-sensitive, we examined an effect of a protonophorous uncoupler monensin known to exchange H^+ for alkali cations (Na^+ in particular) across the membranes. This antiporter belongs to the group of ionophores, such as nigericin, which prevent formation of the light-induced ΔpH in thylakoids and reverse nonphotochemical quenching of

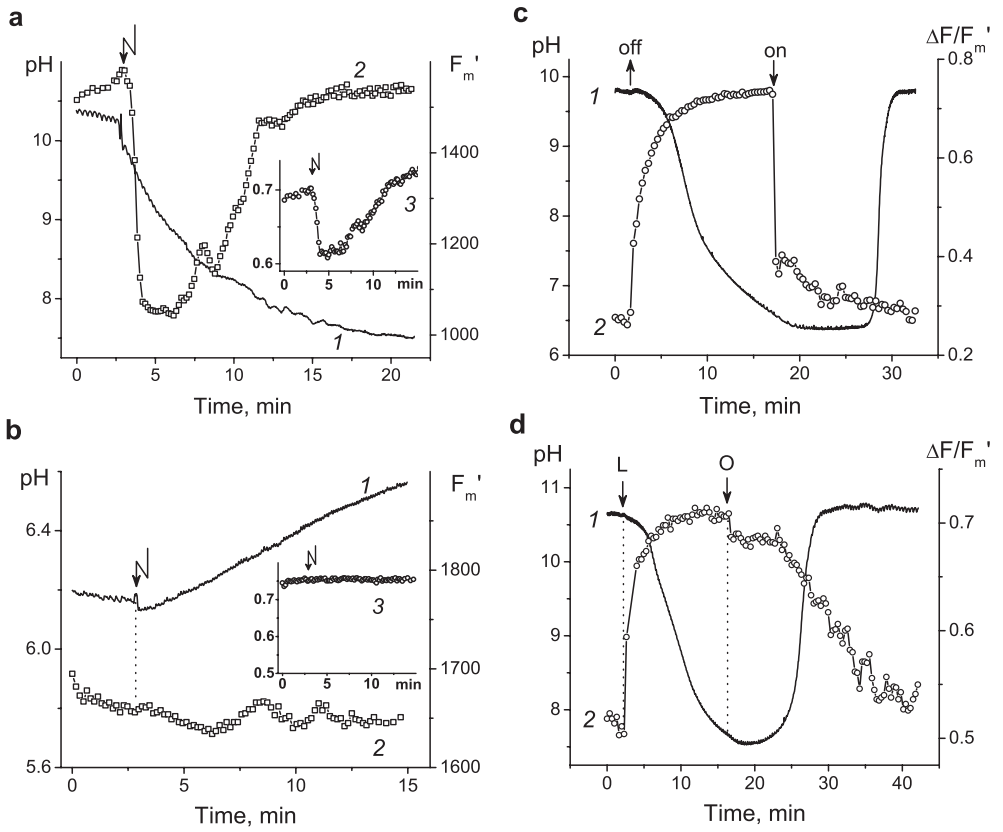

Fig. 2. Simultaneous measurements of pH, chlorophyll fluorescence, and quantum yield of PSII electron flow in the alkaline and acid regions of *Chara* cells after electric excitation and alteration of light conditions. (a, b) Local changes in pH_o (solid lines 1), maximal fluorescence F_m' (2), and effective quantum yield of PSII electron flow $\Delta F/F_m'$ (insets, 3) in the alkaline (a) and acidic (b) cell regions after AP generation. Cells were exposed to blue light with fluence rates of 6.0 (a) and 3.3 μmol m^{-2} s^{-1} (b). (c, d) Changes in pH_o (1) and effective quantum yield of PSII electron flow, $\Delta F/F_m'$ (2) in the alkaline cell regions upon light–dark transition (c) and after transition from overall to local illumination of equal intensity (d). Blue light with intensities of 30 μmol m^{-2} s^{-1} (c) and 12 μmol m^{-2} s^{-1} (d). Upward and downward arrows designate light off and light on treatments; arrows L and O designate transitions to local illumination (d=2.5 mm) and the return to overall illumination, respectively.

chlorophyll fluorescence in leaves and chloroplasts [27]. Effects of monensin and nigericin on the electric responses of *Anthoceros* plant cells to light were similar [4]. As shown in Fig. 3d, strong nonphotochemical quenching (low F_m') was imposed by light in the alkaline cell region, which was released on darkening. In the presence of 10 μM monensin, illumination produced no quenching and even raised F_m' slightly. The loss of sensitivity to light after monensin treatment is in contrast to a large light-induced drop in F_m' in untreated cells. Clearly, the light-induced nonphotochemical quenching in *Chara* is related to ΔpH gradient at thylakoid membranes.

3.4. Effect of action potential on photosynthetic oxygen evolution

The decrease in $\Delta F/F_m'$ after AP indicates transient inhibition of noncyclic electron flow and implies that photosynthetic O_2 evolution should be affected by membrane excitation. Fig. 4 shows local changes in O_2 content in the alkaline zone induced by AP. The AP generation caused a transient decrease in O_2 content (solid line 1), which had a marked similarity with the decrease in $\Delta F/F_m'$ (curve 2, symbols). The amplitudes of excitation-induced decrease in O_2 content constituted about one-fourth of the changes produced by switching on and off the actinic light (30 μmol^{-2} s^{-1}). The excitation-induced pO_2 signals were smaller by a factor of 2.5–4 in the acidic zones than in the alkaline zones. The reversible suppression of pO_2 signal by AP could be observed irrespective of whether the alkaline band had restored after the previous excitation.

4. Discussion

Two phenomena induced by the PM excitation in *Chara*–temporal suppression of pH bands and photosynthesis in the alkaline cell regions–seem to originate from related though different operational pathways that have common origin but diverge at later stages. Both pathways are triggered by AP, which involves the increase in cytosolic Ca^{2+} level as a key stage [29,30] and the activation of Ca^{2+}-gated Cl^- and K^+ channels [10]. The increase in $[Ca^{2+}]_{cyt}$ during AP might be a common signal for both pathways, whereas fluxes of Cl^- and K^+ can hardly affect cytosolic concentrations that are 5–6 orders of magnitude higher than $[Ca^{2+}]_{cyt}$. The elevation of Ca^{2+} level in the plant cell cytoplasm occurs immediately

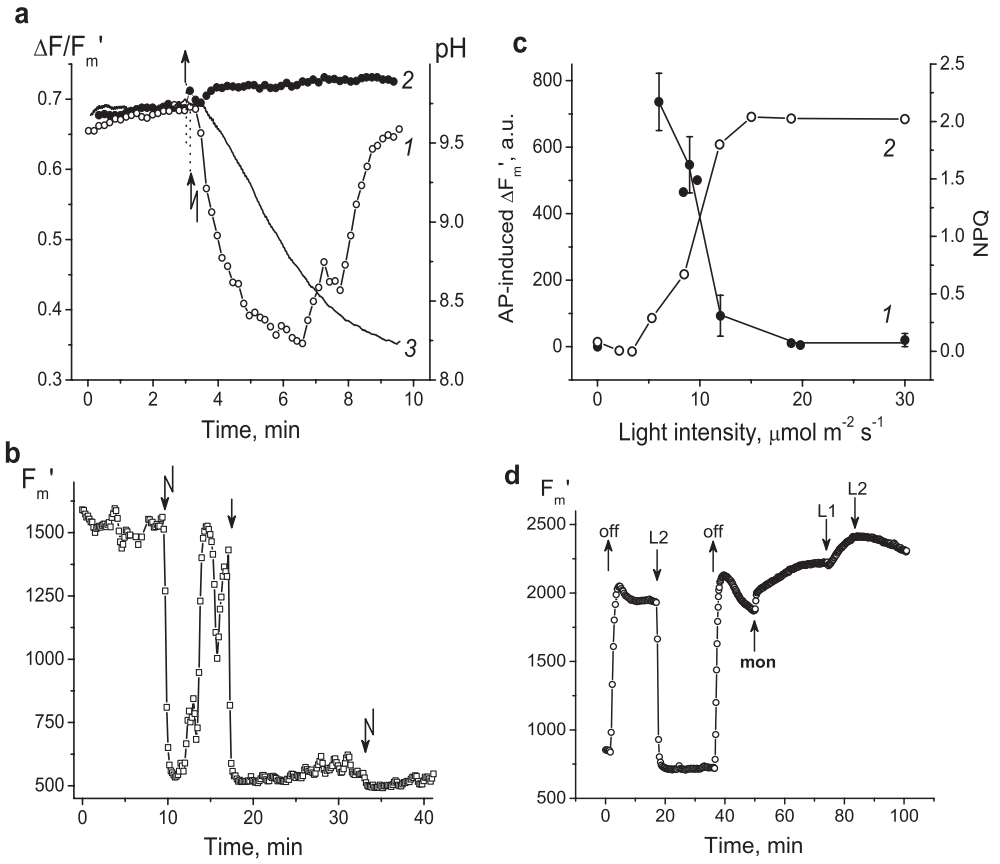

Fig. 3. Light requirements of excitation-induced fluorescence quenching and sensitivity of quenching to a protonophore. (a) Changes of $\Delta F/F_m'$ induced in the alkaline cell region by triggering AP in the light (curve 1, open symbols) and 10 s after darkening (curve 2, filled symbols). Solid line 3 shows the decay of alkaline band induced by triggering AP 10 s after darkening. Blue light, 8.4 μmol m^{-2} s^{-1}. Upward arrow refers to records 2 and 3 only and marks the moment when light was switched off. (b) Complementary relations between light-induced and AP-induced F_m' quenching, revealed from AP-induced F_m' changes at light intensities of 8.4 and 30 μmol m^{-2} s^{-1}. A downward arrow corresponds to the increase in light intensity. (c) Amplitude of AP-induced changes in F_m' (filled symbols, 1) and sustained nonphotochemical quenching NPQ (open symbols, 2) as functions of actinic light intensity. Bars represent standard errors of the means with n ranging from 3 to 6. (d) Elimination of light-induced F_m' quenching by 10 μM monensin. Changes in F_m' were induced by darkness (off), monensin addition (mon), and illumination at photon flux densities of 12 and 30 μmol m^{-2} s^{-1} (arrows L1 and L2, respectively).

during AP and with a delay of few minutes after light–dark transitions [31]. This might account for the time-shifted kinetics of AP- and dark-induced pH and MP changes (Fig. 1). There is ample evidence that cytosolic Ca^{2+} affects ion pumps and channels in plant cells in both direct and indirect ways [5,32].

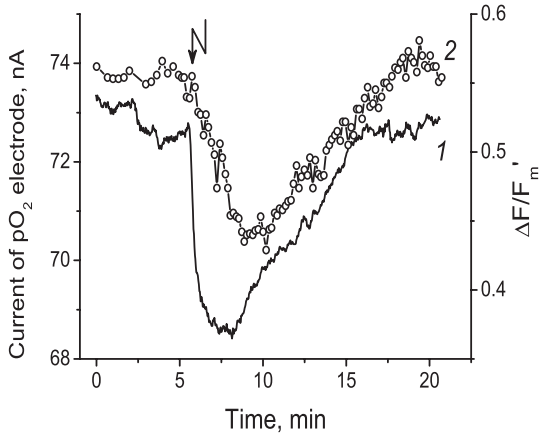

Fig. 4. Changes in the electrode current of pO_2 sensor (solid line 1) and the effective quantum yield of PSII electron flow, $\Delta F/F_m'$ (2) in the alkaline regions of *Chara* cell upon electro-stimulated AP generation. Fluence rate 8.4 μmol m^{-2} s^{-1}.

The excitation effects reported here develop in the time range from seconds to tens of minutes. These AP-induced events are not strictly linked and differ in light requirements and other features. (i) The effect of AP on pH bands is light independent in strict sense, as photosynthesis is needed only for band formation. If the band pattern was preformed, AP eliminated pH bands regardless of light exposure at a moment of excitation. By contrast, the AP effect on F_m' and $\Delta F/F_m'$ disappeared if the interval between the onset of darkness and AP was as short as 10 s. Hence, photosynthetic electron flow was required for the action of AP on F_m' and $\Delta F/F_m'$. (ii) The pH pattern smoothes or vanishes after AP, whereas the photosynthetic pattern becomes even more pronounced. Although we did not measure spatial profiles for F_m' and $\Delta F/F_m'$ in this work, our data clearly show that F_m' and $\Delta F/F_m'$ are insensitive to AP in the acid regions but diminish in alkaline regions. This means that the difference between these regions in terms of F_m' and $\Delta F/F_m'$ increases after AP generation. (iii) Effects of AP on PM, reflected by changes

in pH_o and MP, are phenomenologically similar to the effect of darkness, whereas the action of AP on F_m' and $\Delta F/F_m'$ is similar to the effect of strong light.

The similarity in PM events induced by AP and darkening is evident in Fig. 1. Both treatments depressed pH_o to similar extents in the alkaline zones. Likewise, both AP and darkness induced hyperpolarization, but the MP response to darkness was delayed compared to post-excitation hyperpolarization. Previous study of electrogenesis in *Chara* proved that the plasmalemma in alkaline regions of illuminated cells is depolarized due to high H^+ conductance, g_H [26]. The large H^+ (OH^-) conductance of *Chara* plasmalemma at high pH is well known [33]. The hyperpolarization arising upon light–dark transition reflects inactivation of g_H [26]. One may suppose that the AP-induced hyperpolarization is also due to the inactivation of g_H.

The effect of AP on photosynthesis is manifested in changes of $\Delta F/F_m'$, which is a measure of linear electron transport under constant irradiance, as well as in pO_2 changes (Fig. 4). Kinetic similarity of $\Delta F/F_m'$ and pO_2 signals after excitation proves that AP inhibits linear electron flow and retards photosynthetic O_2 evolution. The depression of electron transport after AP was largely due to nonphotochemical quenching in PSII (the increased dissipation of chlorophyll excitations to heat reflected by the decrease in F_m').

Complementary relations between AP-induced changes in F_m' and light-dependent quenching, together with sensitivity of quenching to a protonophore (Fig. 3), indicate that nonphotochemical quenching after AP is related to the formation of thylakoid ΔpH and low lumen pH. In contrast to state transitions and photoinhibition, the AP-induced quenching developed fast (0.5–1 min after AP) and was most pronounced at low-intensity light.

A hypothetical vision of AP-induced increase in thylakoid ΔpH should take into account the increase in $[Ca^{2+}]_{cyt}$ during AP, light-dependent Ca^{2+} uptake by chloroplasts [34,35], effects of Ca^{2+} on Calvin cycle [36], and operation of Ca^{2+}/H^+ antiporter at the thylakoid membranes [37]. These factors may affect the thylakoid ΔpH and linear electron flow, as documented by rapid decrease in $\Delta F/F_m'$ and F_m'.

Further studies should clarify why AP had strong influence on photosynthesis in chloroplasts of alkaline but not of acidic cell regions. It should be noted that the rise in $[Ca^{2+}]_{cyt}$ after AP is likely superimposed on opposite changes in cytosolic pH, because AP suppressed counter-directed H^+ fluxes in the alkaline and acid regions. Finally, it appears that excitation-induced events at PM and in the chloroplast originate from a common cause but proceed through divergent reaction pathways.

Acknowledgments

This work was supported by the Russian Foundation for Basic Research. We are grateful to Prof. W.J. Vredenberg from Wageningen University and the Netherlands Organization for Scientific Research (NWO) for the instrumental support.

References

[1] T. Sibaoka, Physiology of rapid movements in higher plants, Annu. Rev. Plant Physiol. 20 (1969) 165–184.
[2] D. Hodick, A. Sievers, The action potential of *Dionaea muscipula* Ellis, Planta 174 (1988) 8–18.
[3] K. Trebacz, T. Zawadski, Light-triggered action potentials in the liverwort *Conocephalum conicum*, Physiol. Plant. 64 (1985) 482–486.
[4] A.A. Bulychev, W.J. Vredenberg, Enhancement of the light-triggered electrical response in plant cells following their deenergization with uncouplers, Physiol. Plant. 94 (1995) 64–70.
[5] S. Zimmermann, T. Ehrhardt, G. Plesch, B. Mueller-Rober, Ion channels in plant signaling, Cell. Mol. Life Sci. 55 (1999) 183–203.
[6] E.P. Spalding, Ion channels and the transduction of light signals, Plant Cell Environ. 23 (2000) 665–674.
[7] V.A. Shepherd, M.J. Beilby, T. Shimmen, Mechanosensory ion channels in charophyte cells: the response to touch and salinity stress, Eur. Biophys. J. 31 (2002) 341–355.
[8] E. Krol, H. Dziubinska, K. Trebacz, Low-temperature induced transmembrane potential changes in the liverwort *Conocephalum conicum*, Plant Cell Physiol. 44 (2003) 527–533.
[9] D.C. Wildon, J.F. Thain, P.E.H. Minchin, I.R. Gubb, A.J. Reilly, Y.D. Skipper, H.M. Doherty, P.J. O'Donnell, D.J. Bowles, Electrical signalling and systemic proteinase inhibitor induction in the wounded plant, Nature 360 (1992) 62–65.
[10] V.S. Lunevsky, O.M. Zherelova, I.Y. Vostrikov, G.N. Berestovsky, Excitation of Characeae cell membranes as a result of activation of calcium and chloride channels, J. Membr. Biol. 72 (1983) 43–58.
[11] M. Wacke, G. Thiel, Electrically triggered all-or-none Ca^{2+}-liberation during action potential in the giant alga *Chara*, J. Gen. Physiol. 118 (2001) 11–21.
[12] C. Koziolek, T.E.E. Grams, U. Schreiber, R. Matyssek, J. Fromm, Transient knockout of photosynthesis mediated by electric signals, New Phytol. 161 (2003) 715–722.
[13] T. Shimmen, T. Mimura, M. Kikuyama, M. Tazawa, Characean cells as a tool for studying electrophysiological characteristics of plant cells, Cell Struct. Funct. 19 (1994) 263–278.
[14] M. Wacke, G. Thiel, M.-T. Hutt, Ca^{2+} dynamics during membrane excitation of green alga *Chara*: model simulations and experimental data, J. Membr. Biol. 191 (2003) 179–192.
[15] M. Tazawa, Cell physiological aspects of the plasma membrane electrogenic H^+ pump, J. Plant Res. 116 (2003) 419–442.
[16] W.J. Lucas, The influence of light intensity on the activation and operation of the hydroxyl efflux system of *Chara corallina*, J. Exp. Bot. 26 (1975) 347–360.
[17] W.J. Lucas, R. Nuccitelli, HCO_3^- and OH^- transport across the plasmalemma of *Chara*: spatial resolution obtained using extracellular vibrating probe, Planta 150 (1980) 120–131.
[18] J.M. Fisahn, U.-P. Hansen, W.J. Lucas, Reaction kinetic model of a proposed plasma membrane two-cycle H^+-transport system of *Chara corallina*, Proc. Natl. Acad. Sci. U. S. A. 89 (1992) 3261–3265.
[19] T. Shimmen, A. Yamamoto, Induction of a new alkaline band at a target position in internodal cells of *Chara corallina*, Plant Cell Physiol. 43 (9) (2002) 980–983.
[20] C. Plieth, H. Tabrizi, U.-P. Hansen, Relationship between banding and photosynthetic activity in *Chara corallina* as studied by the spatially different induction curves of chlorophyll fluorescence observed by an image analysis system, Physiol. Plant. 91 (1994) 205–211.
[21] A.A. Bulychev, A.A. Cherkashin, A.B. Rubin, W.J. Vredenberg, V.S. Zykov, S.C. Mueller, Comparative study on photosynthetic activity of chloroplasts in acid and alkaline zones of *Chara corallina*, Bioelectrochemistry 53 (2001) 225–232.
[22] A.A. Bulychev, W.J. Vredenberg, Spatio-temporal patterns of photosystem II activity and plasma-membrane proton flows in *Chara corallina* cells exposed to overall and local illumination, Planta 218 (2003) 143–151.
[23] I. Foissner, Microfilaments and microtubules control the shape, motility, and subcellular distribution of cortical mitochondria in characean internodal cells, Protoplasma 224 (2004) 145–157.

[24] A.A. Bulychev, N.A. Kamzolkina, J. Luengviriya, A.B. Rubin, S.C. Mueller, Effect of a single excitation stimulus on photosynthetic activity and light-dependent pH banding in *Chara* cells, J. Membr. Biol. 202 (2004) 11–19.
[25] C.-H. Goh, U. Schreiber, R. Hedrich, New approach to monitoring changes in chlorophyll a fluorescence of single guard cells and protoplasts in response to physiological stimuli, Plant Cell Environ. 22 (1999) 1057–1070.
[26] S.A. Frost Shartzer, J.M. Fisahn, W.J. Lucas, Simultaneous measurement of extracellular current and membrane potential of *Chara corallina* internodal cells during light-induced modulation of H^+ transport, C. R. Acad. Sci. Paris. Ser. III 315 (1992) 247–254.
[27] V.R. Ruban, P. Horton, An investigation of the sustained component of nonphotochemical quenching of chlorophyll fluorescence in isolated chloroplasts and leaves of spinach, Plant Physiol. 108 (1995) 721–726.
[28] P. Mueller, X.-P. Li, K. Niyogi, Non-photochemical quenching. A response to excess light energy, Plant Physiol. 125 (2001) 1558–1566.
[29] M. Kikuyama, M. Tazawa, Temporal relationship between action potential and Ca^{2+} transient in characean cells, Plant Cell Physiol. 39 (1998) 1359–1366.
[30] G. Thiel, M. Wacke, I. Foissner, Ca^{2+} mobilization from internal stores in electrical membrane excitation in *Chara*, Prog. Bot. 64 (2002) 217–233.
[31] J. Sai, C.H. Johnson, Dark-stimulated calcium ion fluxes in the chloroplast stroma and cytosol, Plant Cell 14 (2002) 1279–1291.
[32] T. Kinoshita, M. Nishimura, K. Shimazaki, Cytosolic concentration of Ca^{2+} regulates the plasma membrane H^+-ATPase in guard cells of fava bean, Plant Cell 7 (1995) 1333–1342.
[33] M.A. Bisson, N.A. Walker, The *Chara* plasmalemma at high pH. Electrical measurements show rapid specific passive uniport of H^+ or OH^-, J. Membr. Biol. 56 (1980) 1–7.
[34] S. Muto, S. Izawa, S. Miyachi, Light-induced Ca^{2+} uptake by intact chloroplasts, FEBS Lett. 139 (1982) 250–254.
[35] G. Kreimer, M. Melkonian, E. Latzko, An electrogenic uniport mediates light-dependent Ca^{2+} influx into intact spinach chloroplasts, FEBS Lett. 180 (1985) 253–258.
[36] R.A. Wolosiuk, C.M. Hertig, A.N. Nishizawa, B.B. Buchanan, Enzyme regulation in C_4 photosynthesis. Role of Ca^{2+} in thioredoxin-linked activation of sedoheptulose bisphosphatase from corn leaves, FEBS Lett. 140 (1982) 31–35.
[37] W.F. Ettinger, A.M. Clear, K.J. Fanning, M.L. Peck, Identification of Ca^{2+}/H^+ antiport in the plant chloroplast thylakoid membrane, Plant Physiol. 119 (1999) 1379–1385.